ELSEVIER

Biochimica et Biophysica Acta 1510 (2001) 426–441

BIOCHIMICA ET BIOPHYSICA ACTA
BBA

www.elsevier.com/locate/bba

Vesicular monoamine transporters heterologously expressed in the yeast *Saccharomyces cerevisiae* display high-affinity tetrabenazine binding

Rodrigo Yelin, Shimon Schuldiner *

Alexander Silberman Institute of Life Sciences, Hebrew University, Givat Ram, Jerusalem 91904, Israel

Received 21 July 2000; received in revised form 26 October 2000; accepted 9 November 2000

Abstract

A mammalian vesicular neurotransmitter transporter has been expressed in the yeast *Saccharomyces cerevisiae*. The gene encoding the rat vesicular monoamine transporter ($rVMAT_1$) was cloned in several expression plasmids. The transporter was expressed at detectable levels only when short sequences using codons favored by *S. cerevisiae* were fused preceding the start of translation of $rVMAT_1$. The scarce expression of the wild-type protein was, most likely, due to the fact that part of the N-terminus of the protein is encoded by codons not preferred in *S. cerevisiae*. Furthermore, low growth temperatures increased $rVMAT_1$ expression and altered its processing. Whereas at 30°C the protein is not glycosylated, at lower temperatures ($\sim$16°C) half of the expressed transporters undergo core glycosylation. In addition, under these conditions the levels of protein expression significantly increase. Using a functional chimeric protein composed by VMAT and the green fluorescent protein (GFP), it is shown that the punctate pattern of intracellular distribution remains invariable at the different temperatures. Using a similar fusion sequence, the bovine VMAT isoform 2 ($bVMAT_2$) was also expressed in yeast. The yeast-expressed $bVMAT_2$ binds [^{3}H]dihydrotetrabenazine ([^{3}H]TBZOH) with the same characteristics found in the native protein from bovine chromaffin granules. Dodecyl maltoside-solubilized $bVMAT_2$ retains the conformation required for [^{3}H]TBZOH binding. We exploited the robust binding to follow the transporter during purification assays on a Ni^{2+}-chelating column. In this report we describe for the first time the heterologous expression of a neurotransmitter transporter in the yeast *S. cerevisiae*.

Keywords: Neurotransmitter transport; Codon usage; Heterologous expression; Protein folding; Tetrabenazine; Vesicular monoamine transporter; Chaperone

1. Introduction

Vesicular neurotransmitter transporters (VNTs) are responsible for the transport of classical neurotransmitters into synaptic vesicles and storage organelles of secretory cells. Vesicular transport activities have been described for acetylcholine, glutamate, γ-aminobutyric acid and glycine [1]. The transport

Abbreviations: 5-HT, serotonin; ADH, alcohol dehydrogenase; HA, hemagglutinin; MPP^+, *N*-methyl-4-phenylpyridinium; PAGE, polyacrylamide gel electrophoresis; PCR, polymerase chain reaction; PBS, phosphate-buffered saline; PGK, phosphoglycerate kinase; PMA1, plasma membrane ATPase; SDS, sodium dodecyl sulfate; VNT, vesicular neurotransmitter transporter; VMAT, vesicular monoamine transporter; $rVMAT_1$, rat vesicular monoamine transporter type 1; $bVMAT_2$, bovine vesicular monoamine transporter type 2; TBS-T, Tween-20 in Tris-buffered saline; TBZOH, dihydrotetrabenazine; TBZ, tetrabenazine

* Corresponding author. Fax: +972-2-563-4625; E-mail: shimons@leonardo.ls.huji.ac.il

0005-2736/01/$ – see front matter
PII: S0005-2736(00)00374-6

of biogenic amines has served as the experimental paradigm, most likely due to the use of bovine chromaffin granules, an abundant source of material with robust transport activity. Transport of the monoamines serotonin, dopamine, norepinephrine, epinephrine, and histamine into storage organelles is catalyzed by the vesicular monoamine transporter (VMAT). VMAT has been purified from chromaffin granules [2–4]. Cloning of VMAT was achieved both by functional expression [5] and using the expression cloning approach [6]. The cloned transporter protects against the toxicity of 1-methyl-4-phenylpyridinium (MPP^+), by sequestering it within a vesicular compartment. Two isoforms of the transporter have been identified: $VMAT_1$ and $VMAT_2$. The isoforms show a high sequence similarity; yet they differ in their pharmacological profile and affinity to histamine. Whereas $VMAT_1$ is nearly insensitive to tetrabenazine (TBZ) inhibition, $VMAT_2$ is inhibited and binds TBZ at concentrations in the nanomolar range [7]. The identification of the genes coding for the transporters allowed the analysis of the role of specific amino acids in the transporter activity [8–11]. In a recent study, we examined the importance of glycosylation and characterized a mutation at a conserved proline residue which affects the folding, localization and activity of VMAT [12].

To further understand the mechanism of transport, high-resolution structure information is required. Purification of proteins from native sources often requires lengthy and laborious procedures. In recent years, the use of tags has simplified purification procedures to 'single-column protocols'. Efficient expression systems are essential for allowing the introduction of suitable purification tags and render large quantities of functional protein. Several heterologous expression systems were developed and are extensively used in modern biochemistry. Among them, the yeast *Saccharomyces cerevisiae*, for which a vast knowledge on its genetics and biochemistry is available, became widely accepted. *S. cerevisiae* has already been successfully used for heterologous expression and cloning of several membrane proteins. For instance, various plant transporters [13–16], mammalian membrane proteins such as the human D_{2S} dopamine receptor [17], the P-glycoprotein [18], the mouse transporter protein (MTP) [19], etc. We have shown recently, that EmrE, a bacterial multidrug transporter, is expressed at high levels in *S. cerevisiae* conferring resistance to a variety of toxicants by sequestration into the vacuole [20]. VMAT is unique in that it is an H^+-substrate antiporter that its default localization in mammalian cells is in storage subcellular organelles such as synaptic vesicles and chromaffin granules. In this report we describe the expression of VMAT in *S. cerevisiae*. We found that the expression of VMAT is highly dependent on several factors, including the coding sequence of the amino terminus and growth temperature. The yeast-expressed $bVMAT_2$ binds [^{3}H]dihydrotetrabenazine ([^{3}H]TBZOH) with the characteristics displayed by the native protein. We exploited the stability of the complex [^{3}H]TBZOH-bVMAT2 to follow the transporter during purification procedures.

2. Materials and methods

2.1. Strains

Bacterial strain *Escherichia coli* DH5α [21] was used for propagation of recombinant plasmids. The *S. cerevisiae* strains used in this study were: YAE65 (MAT a, ade2–119, ilv1–92, trp5-b, sge1, ura3Δ5) and YHE4 (MAT a, ade2–119, ilv1–92, trp5-b, ura3Δ5) [22,23] (kindly supplied from C. Senstag, University of Zurich), BWT-1 (MAT a, his3, lys2, ura3, leu2, trp1, met10, GAL+) [20], YMTAB (MAT α, leu2–3, 112, ura3Δ5, pra1::HIS3, prb1ΔV, GAL+) [17] and SY1 (MAT a, ura3–52, leu2–3,112, his4–619, *sec6–4*, GAL [24] a gift of Professor C. Slayman (Yale University).

2.2. Media

S. cerevisiae strains were grown in standard media. Complete YPD medium (containing 1% yeast extract, 2% bactopeptone, and 2% glucose) was used to grow non-transformed strains. Minimal medium (SD) (0.17% yeast nitrogen base without amino acids (Difco), 0.5% ammonium sulfate and 2% glucose or 2% galactose) was supplemented according with the auxotrophic requirements as described in [25]. Temperature of growth was 30°C unless indicated otherwise. Expression under GAL promoter was checked

either after growth in 2% galactose or after exposing cells which grew using raffinose, lactate or glucose as carbon source to 2% galactose for 2, 4, 8 and 24 h. Yeast cells were transformed using the method of Elble [26].

2.3. Plasmids

The following yeast-expression vectors were used. pAD4Δ is a 2μ plasmid, LEU2, with ADH promoter and terminator [27]. p421 is a 2μ plasmid, LEU2, with PMA1 promoter and terminator [28]. p112 is a CEN4 plasmid, URA3, with GAL1 and GAL10 promoters [29]. p413Gal is a CEN4 plasmid derived from p413 [30] with the GAL1 promoter inserted at the Sal I site. BFG-1 is a 2μ plasmid, PGK promoter and terminator, LEU2; it contains an ATG site for start of translation, followed by three copies of the hemagglutinin (HA) epitope [31], see Fig. 1A. Canine calnexin [32], a generous gift from Dr C. Tate (MRC Laboratory of Molecular Biology, Cambridge, UK), was expressed under the GPD promoter of the pG-1 plasmid [33]. SHR3 was expressed using the plasmid pPL250 from [34] kindly provided by Dr Per Ljungdahl (Ludwig Institute for Cancer Research, Sweden). For stable transfection of CHO cells, pCIN plasmid allows for stable transfection of cells based on selection with neomycin [35].

2.4. Cloning procedures

The cDNA of $rVMAT_1$ was excised from pTMI/$rVMAT_1$ [8] with *Eco*RI and *Xho*I and inserted in pBluescript KS at the same sites creating an intermediate plasmid pBS/$rVMAT_1$. This plasmid contains the *Eco*RI site immediately before the ATG that starts the translation of $rVMAT_1$ and the entire 3′ untranslated region (592 bases) [5]. To insert $rVMAT_1$ in the plasmid pAD4Δ [27], pBS/$rVMAT_1$ was partially digested with *Pst*I and a fragment

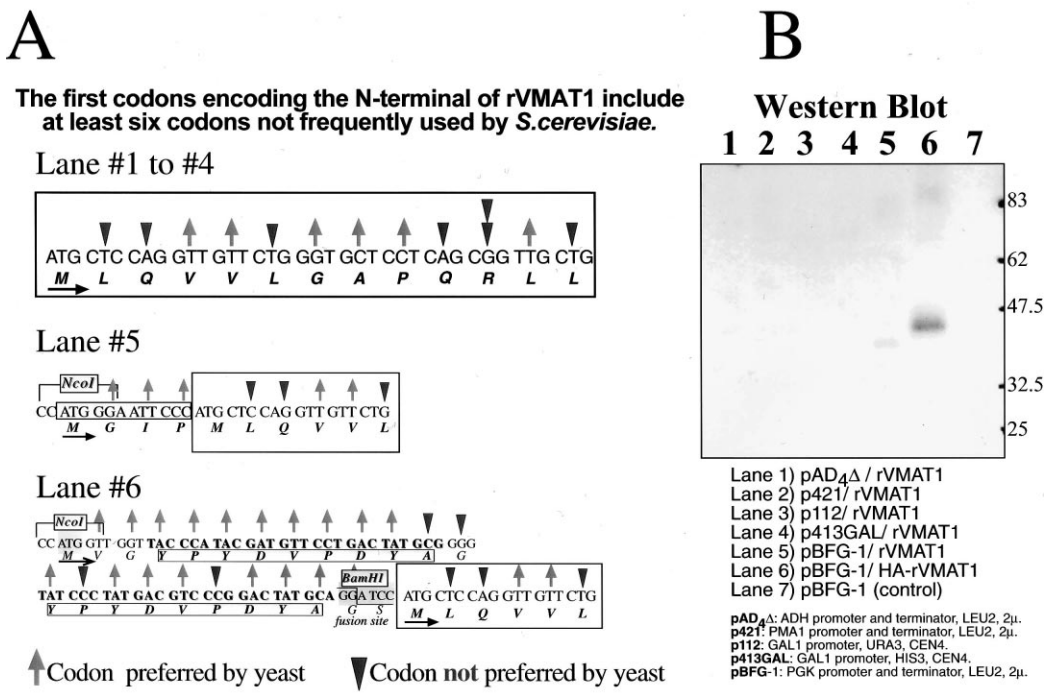

Fig. 1. The codon usage at the amino terminus affects the levels of $rVMAT_1$ expression. (A) The first 13 amino acids and the coding sequence is shown in the upper box. Codons preferred by yeast [36] are shown with up-arrows, while seldom-used codons are shown with inverted triangles. The middle box shows to the short sequence fused to $rVMAT_1$ (lane 5). The lower box (lane 6) shows the longer sequence fused; the HA-epitope (repeated twice) and the fusion site are highlighted. (B) Total membranes prepared from *S. cerevisiae* transformed with the indicated constructs were separated and immunoblotted using an antibody raised against the C-terminus of $rVMAT_1$ [5]. Similar amounts of protein were loaded onto the gel.

containing the coding region of $rVMAT_1$ and the first 281 bases of the 3′-UTR was used for ligation. $rVMAT_1$ was inserted at the *Pst*I site of pAD4Δ and the orientation was verified with several restriction enzymes. In the proper orientation, the ATG which starts the translation is located 10 bases from the cloning site. To insert $rVMAT_1$ in p112 [29], $rVMAT_1$ was excised from pBS/$rVMAT_1$ with *Bam*HI and *Xho*I and inserted in p112 previously digested with *Bam*HI and *Sal*I. As a result, the ATG is located 26 bases downstream the *Bam*HI site and 70 bases from the 5′-end of the mRNA transcript. A second intermediate plasmid (pBS/$rVMAT_1$-B) was constructed by partial digestion of pBS/$rVMAT_1$ with *Pst*I and insertion at the same site of pBluescript KS. In pBS/$rVMAT_1$-B the ATG (start of translation) is located near the *Xho*I site of the pBluescript multicloning site. To insert $rVMAT_1$ in p421 [28], pBS/$rVMAT_1$-B was digested with *Xho*I and *Bam*HI and the plasmid with *Xho*I and *Bgl*II. Accordingly, the ATG is located 50 bases from the *Xho*I cloning site. pBS/$rVMAT_1$-B was digested with *Sal*I and *Not*I and inserted in p413Gal at the same sites. In p413Gal/$rVMAT_1$, the ATG is located 50 bases from the *Sal*I site.

All PCR-derived sequences were checked for the absence of point mutations. The insert from pTMI/$rVMAT_1$ [8] was digested with *Xho*I and partially digested with *Nco*I, and inserted in BFG-1 at the same sites; in this construct (BFG-1/$rVMAT_1$) the translation starts from the ATG within the *Nco*I site of BFG-1. In this case, three amino acids encoded with codons preferred by yeast; e.g., codons utilized for highly-expressed endogenous proteins [36] precede the first amino acid of $rVMAT_1$. To create BFG-1/HA-$rVMAT_1$, a PCR product using oligonucleotides PGK-$rVMAT_1$ and RP2421 (all oligonucleotides sequences are shown in Table 1) was inserted in frame at the first *Bam*HI site of BFG-1 (see sequence below and in Fig. 1A). The oligonucleotide used places a *Bam*HI site immediately before the ATG start of translation of $rVMAT_1$. As a result $rVMAT_1$ contains additional 24 amino acids at its amino terminus comprising two copies of the HA epitope (YPYDVPDYA) [37]. Addition of the six-histidine tag (His_6 tag) at the carboxy terminus of $rVMAT_1$ was done using PCR with primers PGK-$rVMAT_1$ and a reverse primer designed for this purpose (RP-His Tag-$rVMAT_1$). This primer introduces an *Eco*RI site followed by six histidines immediately before the stop codon of $rVMAT_1$. Therefore, the His_6 tag tail comprises eight residues: phenylalanine

Table 1
Oligonucleotides used in this investigation

Name	Purpose		Oligonucleotide sequence
PGK-$rVMAT_1$	Insertion of $rVMAT_1$ in frame in plasmid BFG-1 at *Bam*HI site	Sense	5′-TTGAATTCGTCGACGGATCC***ATG***CTCCAGGTTGTTC
RP-HisTag-$rVMAT_1$	Addition of His_6 tag to the C-terminus of $rVMAT_1$	Antisense	5′-CCATCGATGATATCTTAATGATGATGATGATG-ATGGAATTCCTCCCCGCTGCTAGGATC
PGK-$bVMAT_2$	Insertion of $rVMAT_1$ in frame in plasmid BFG-1 at *Not*I site	Sense	5′-TATAGAGCTCGCGGCCGC***ATG***GCCCTGAGCGAG
RP-$bVMAT_2$	Inserts *Eco*RI site before the stop codon to allow insertion of the His_6 tag engineered for $rVMAT_1$	Antisense	5′-CCGCTCGAGTTAGAATTCGTCACTTTCAGATTCTTCATCC
RP 2421	Adds restriction sites to 3′-UTR of $rVMAT_1$ for cloning in different vectors	Antisense	5′-CGAGATCTGAATTCCTCGAGATCCATTGTGC
HA-pCIN	Allows insertion of 5′-end of HA-tagged genes in plasmid pCIN	Sense	5′-CGCTCTAGATCGATCGCGGCCGCC***ATG***GTTGGTTACCCATAC
RP-pCIN	Allows insertion of genes bearing the 3′-UTR of $rVMAT_1$ in plasmid pCIN	Antisense	5′-GCTGAGATCTGAATTCGCTAGCTCGAGATCCATTGTGC

Start of translation sequence is shown with bold, underlined, italicized letters (***ATG***).

and glutamate corresponding to the *Eco*RI site, and six histidine of the tag. Similarly, BFG-1/HA-bVMAT$_2$-His was created after in frame insertion of the coding region of bVMAT$_2$ at the *Not*I and *Xho*I sites of BFG-1 using primers PGK-bVMAT$_2$ and RP-bVMAT$_2$. This construct was next digested with *Eco*RI and *Xho*I and the His$_6$ tag tail (including the 3′-UTR of rVMAT$_1$) from plasmid BFG-1/HA-rVMAT$_1$-His was inserted creating BFG-1/HA-bVMAT$_2$-His. HA-bVMAT$_2$-His contains 38 additional amino acids at the amino terminus, accommodating three copies of the HA epitope. The DNA sequence of the coding region of BFG-1 is: 5′-***CCATGG***TTGGTTACCCATACGATGTTCCTGACTATGCGGGCTATCCCTATGACGTCCCGGACTATGCA***GGATCC***TATCCATATGACGTTCCAGATTACGCTGCTCAGT***GCGGCCGC***-3′. The first, second and third bold-italicized sequences correspond to the *Nco*I, *Bam*HI and *Not*I restriction sites respectively; the first ATG is within the *Nco*I site. The underlined sequences code for HA epitope. For more information see Fig. 1A and [37]. HA-rVMAT$_1$-His was cloned in the pCIN vector using a PCR product prepared using oligonucleotides HA-pCIN and RP-pCIN cleaved with *Not*I and *Bgl*II. The vector pCIN was digested with *Not*I and *Bam*HI and ligated creating pCIN/HA-rVMAT$_1$-His. pCIN/bVMAT$_2$-His was constructed after removing the insert from BFG-1/HA-bVMAT$_2$-His with *Not*I and *Psh*AI and reinserting it in pCIN/HA-rVMAT$_1$-His digested with the same sites (*Psh*AI has a unique recognition site at the 3′-UTR of rVMAT$_1$). As a result, bVMAT$_2$-His looses the amino acids added at the amino terminus but preserves the His$_6$ tag. The chimeric proteins HA-rVMAT$_1$-GFP and HA-bVMAT$_2$-GFP were constructed after exchanging the His$_6$ tag with the gene encoding the green fluorescent protein (GFP, mutant S65T) [38] excised from pRSETb/GFP with *Eco*RI and *Xho*I [39]. The GFP is, thus, inserted in frame at the *Eco*RI site. Canine calnexin (GenBank accession number X53616) inserted in pBluescript II KS at *Bam*HI/*Xba*I sites was excised with *Sac*I and *Eco*RV, blunt-ended with mung bean nuclease and reinserted in pBluescript KS at the *Eco*RV site creating pBS/calnexin. The orientation chosen is the one in which the 5′ of calnexin is located near the *Bam*HI site of the plasmid. Calnexin was removed from pBS/calnexin with *Bam*HI and *Sal*I and inserted in pG-1 [33] at the same sites.

2.5. Preparation of total yeast membranes

The protocols used here were described elsewhere [20].

2.6. Western blot

Blots were performed as described in [37]. Antibody dilutions were as follows: 1:5000 for either monoclonal antibody against the HA epitope (12CA5, from Berkeley Antibodies Co., BAbCo, Berkeley, CA) or polyclonal antibody against C-terminus of rVMAT$_1$ [5]. The antibody against calnexin (from Stressgen, Victoria, British Columbia, Canada) was diluted 1:10 000.

2.7. Stable transfection of CHO cells

The protocol was described in [12]. Individual colonies were isolated and tested for MPP^+ resistance, protein expression and binding of [^{3}H]TBZOH.

2.8. Preparation of CHO membranes

CHO/bVMAT$_2$-His (this work) or CHO/HA-rVMAT$_1$-His [37] cells were seeded on 15-cm culture plates and grown in the presence of 1 mM MPP^+ to ensure elevated VMAT expression. When cultures reached the highest confluence possible (80–90%) cells were harvested either by addition of 25 mM Na_2EDTA in phosphate-buffered saline (PBS) or scrapped with a rubber policeman in the presence of antiproteases [20]. Cells were collected 3000×*g*/5 min/4°C and stored at −70°C prior to use. Membranes were prepared as follows, the frozen pellet was rapidly thawed at 37°C and resuspended in 3 ml of lysis buffer (0.3 M sucrose, 10 mM Tris–Hepes (pH 7.4), 5 mM $MgCl_2$). Cells were disrupted with 20 strokes of a tight pestle-Dounce glass homogenizer. After spinning the suspension (3000×*g*/5 min/4°C) supernatant was saved and unbroken cells were resuspended as before, homogenized and pelleted again. The supernatants were combined and subjected to ultracentrifugation (300 000×*g*/30 min/

4°C), the membranes were resuspended in lysis buffer and used the same day.

2.9. Transient expression in CV-1 cells and preparation of membranes

The methods used in this work, as well as growth conditions and protocols, were described in detail in [12].

2.10. Vacuolar stain with FM4–64

The staining with FM4–64, preparation of slides and visualization in the confocal microscope were described in [20]. Z-Sections of HA-rVMAT$_1$-GFP expressing cells were projected to show the punctate pattern present in the entire cell. The signal corresponding to the GFP fluorescence is shown in the green channel, whereas the signal of the FM4–64 fluorescence is shown in the red channel.

2.11. Binding of [^{3}H]TBZOH to membranes

α-[2-^{3}H]Dihydrotetrabenazine was purchased from American Radiolabeled Chemicals (ARC, St. Louis, MO). Binding was performed essentially as described in [40], with minor modifications. In brief, 50–100 μg membranes were diluted in 300 μl of binding buffer (0.3 M sucrose, 10 mM K-Hepes, pH 7.4) containing 3 nM [^{3}H]TBZOH in the absence or presence of excess tetrabenazine (100 μM). Binding was allowed to occur at room temperature for 15 min. To stop the reaction, 4 ml of ice-cold binding buffer supplemented with 100 μM tetrabenazine were added, and samples were immediately filtered on a HAWP filter 0.45 μm pore size (Millipore). Filters were washed twice with 3 ml of the same solution. For pH dependence studies membranes were diluted in ammonium buffer (150 mM NH_4Cl, 20 mM Mes–Tris, 5 mM $MgCl_2$, titrated to the indicated pH) in the presence of 6.6 nM [^{3}H]TBZOH for 30 min at room temperature. Reactions were stopped with 4 ml of ice-cold ammonium buffer (pH 7.4) supplemented with 100 μM TBZ and filtered as described earlier. Scatchard analysis was performed at pH 7.4, with [^{3}H]TBZOH concentration ranging from 1 to 60 nM. Reactions were stopped after 20 min at room temperature.

2.12. Purification of His$_6$-tagged bVMAT$_2$ from yeast membranes

One to 5 ml HA-bVMAT$_2$-His membranes (10 mg protein/ml) were first labeled with [^{3}H]TBZOH as follows. Membranes were diluted in 10 ml ammonium buffer (pH 7.4) containing 20 nM [^{3}H]TBZOH for 15 min at room temperature. Reactions were stopped by centrifugation at 400 000 × *g*/15 min/4°C. The pellet was washed with 6 ml ammonium buffer, and membranes were finally resuspended in 2 ml of buffer. Solubilization was achieved by stepwise addition of dodecyl maltoside (DM) and cholate to final concentrations of 0.5% and 0.25%, respectively. Suspension was cleared 400 000 × *g*/15 min/4°C, and supernatant was allowed to bind to Ni^{2+}-NTA beads previously equilibrated with the same buffer, in the presence of 30 mM imidazole. Binding was allowed for 1 h, with rotation in a cold room. The bead suspension was loaded in a mini-column and the flowthrough was reloaded three times. The column was washed five times with 4 ml of ammonium buffer containing 0.08% DM, 0.04% cholate and 30 mM imidazole. The protein was eluted in the same buffer as above, but supplemented with 200 mM imidazole. Fractions were collected and radioactivity was assessed by liquid scintillation. In parallel, specific bVMAT$_2$ presence in the different fractions was detected using Western blots as described above.

2.13. Binding of [^{3}H]TBZOH to Ni^{2+}-NTA immobilized transporter

Membranes were diluted in ammonium buffer (150 mM NH_4Cl, 1 mM $MgCl_2$, 10 mM Tris–Hepes, pH 7.4) spun at 400 000 × *g*/15 min/4°C and resuspended in 1 ml of the same buffer. Membrane solubilization and binding to Ni^{2+}-NTA beads was performed as described above. The beads were spun 30 s in a microfuge, washed twice with 1 ml ammonium buffer containing 0.08% DM and 0.04% cholate, and divided into aliquots. The beads were washed once with buffered solutions (10 mM Mes–Tris) and allowed to bind [^{3}H]TBZOH (6 nM) at the indicated pH for 30 min at 4°C with rotation. The binding was measured in triplicate and non-specific binding was measured in the presence of 125 μM TBZ. The bind-

ing was stopped after centrifuging the suspension for 30 s. The beads were washed once with 1 ml ammonium buffer containing 0.08% DM and 0.04% cholate, and radioactivity was assessed by liquid scintillation. Since the binding of the transporter to Ni^{2+}-NTA beads is also pH-dependent, one of the triplicates was used to normalize for the amount of transporter bound to the beads. The protein bound to the beads was eluted with 200 mM imidazole. The eluates were mixed with protein sample buffer and separated on an SDS–PAGE gel as described above. HA-bVMAT$_2$-His was detected using immunoblots. Quantitation of the blots was achieved using the MacBas 2.0 software. Results of radioactivity were normalized according to the quantitation results taken the binding at pH 7.4 as control (100% of binding).

3. Results

3.1. The codons chosen at the N-terminus of rVMAT$_1$ are important for expression

Expression of foreign proteins, specially membrane proteins may interfere with the delicate balance of cellular processes and therefore can have deleterious effects on cell viability. For this reason rVMAT$_1$ was first cloned in an array of expression plasmids that allowed us to control the expression. p112 [29] and p413Gal (derived from [30]) are centromeric plasmids in which the expression is under the inducible GAL1 promoter. Regulation of expression is tight; induction of expression is achieved only after removal of glucose from the medium and upon addition of galactose. On the other hand, plasmids p421 [28] and pAD4Δ [27] are multicopy plasmids equipped with strong constitutive promoters. After completion of plasmid construction, yeast strain BWT-1 was transformed with p421/rVMAT$_1$, pAD4Δ/rVMAT$_1$, p112/rVMAT$_1$ and p413Gal/rVMAT$_1$. To study the expression of rVMAT$_1$, yeast transformants carrying p421/rVMAT$_1$ or pAD4Δ/rVMAT$_1$ were grown on glucose media. Cells carrying the rVMAT$_1$ under the GAL1 promoter (p112/rVMAT$_1$ and p413Gal/rVMAT$_1$) were grown directly on 2% galactose, or first grown on glucose, raffinose or acetate, and then the carbon source was replaced by 2% galactose. Expression of rVMAT$_1$ was assessed using a polyclonal antibody directed against the carboxy terminus of the transporter [5]. No immunoreactive material was detected in membranes prepared from cells carrying the rVMAT$_1$ gene cloned in the above expression plasmids. A representative Western blot is shown in Fig. 1B (lanes 1–4). To test whether an intrinsic determinant, located within the rVMAT$_1$ gene was hampering the expression of the transporter, the codon usage of the 5′ end of rVMAT1 was examined. The use of synonymous codons is strongly biased in the yeast *S. cerevisiae*. Following the cloning of the first glycolytic enzymes, it became clear that yeast evolution changed gene codons in a way where major codons replaced minor codons in highly expressed proteins, and vice versa [36]. In addition, it was shown that replacing an increasing number of major codons with synonymous minor ones at the 5′ end of the coding sequence caused a dramatic decline of the expression level of phosphoglycerate kinase [41]. Examination of the codon usage at the 5′ end of rVMAT$_1$ reveals a trend of minor codons rarely used in *S. cerevisiae* [36,42]. The first 13 codons encoding the N-terminus include at least six that are seldom utilized in yeast for highly expressed proteins (see Fig. 1A, upper box). To test the possibility that the codon usage was impeding the expression of rVMAT$_1$, we fused readily translatable short sequences before the natural start of translation. First, we fused a sequence coding four amino acids using codons favored by yeast (see Fig. 1A, middle box). This addition notably changed the expression of rVMAT$_1$, and a single polypeptide with an apparent size of 45 kDa became easily detectable on immunoblots (Fig. 1B, lane 5). Following this rationale a longer sequence of 24 amino acids was fused, creating HA-rVMAT$_1$. The fused sequence includes two copies of the hemagglutinin (HA) epitope (YPYDVPDYA). The longer fusion further increased the level of expression of rVMAT$_1$ by at least one order of magnitude (see Fig. 1B, lane 6). Importantly, we found no expression from a BFG-1 plasmid bearing the HA-rVMAT$_1$ fusion but lacking the 3′ untranslated region (3′-UTR) of rVMAT$_1$ (not shown). The 3′-UTR probably stabilizes the mRNA transcript allowing efficient expression.

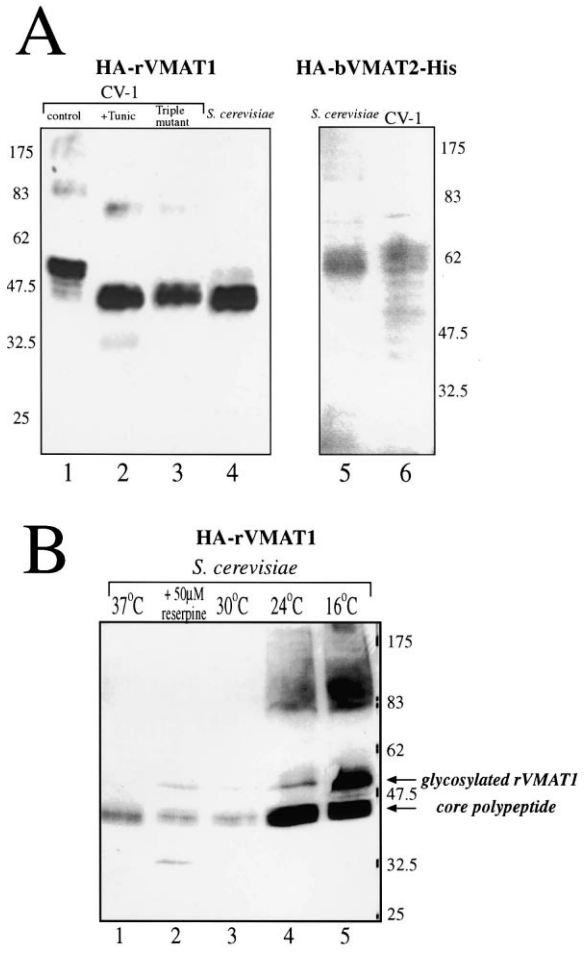

Fig. 2. (A) Yeast-expressed $rVMAT_1$ displays the mobility of the non-glycosylated protein. Membranes were prepared from *Vaccinia*-infected CV-1 cells (monkey kidney fibroblasts) transfected with $rVMAT_1$ (lanes 1 and 2) and $bVMAT_2$ (lane 6). In both cases the HA epitope was fused to the N-terminus as described in Fig. 1. The $rVMAT_1$ protein expressed in the presence of the glycosylation inhibitor tunicamycin is shown in lane 2. In lane 3, a 'Triple' of $rVMAT_1$ devoid of all canonical glycosylation sites is shown [12]. Membranes prepared from *S. cerevisiae* grown at 30°C expressing $rVMAT_1$ or $bVMAT_2$ are shown in lanes 4 and 5, respectively. The samples were immunoblotted with a monoclonal antibody against the HA epitope. (B) $rVMAT_1$ undergoes core glycosylation at low growth temperatures. *S. cerevisiae* was grown at different temperatures and the effect on $rVMAT_1$ expression and processing was tested. Membranes prepared from cells grown at 16°C, 24°C, 30°C and 37°C were separated on a Laemmli 9% gel and immunoblotted using a monoclonal antibody against the HA epitope. Note the increase in the level of expression and the appearance of glycosylated $rVMAT_1$ at low growth temperatures (16°C, lane 5). Addition of the ligand reserpine during the growth step did not influence $rVMAT_1$ expression or processing (lane 2). Similar lack of effect was detected with other substrates of transport: noradrenaline and serotonin (not shown).

3.2. The yeast-expressed $rVMAT_1$ displays the size of the unglycosylated transporter

Addition of epitopes has potentially deleterious effect on protein function. We have already shown that when the tagged transporter is expressed in a mammalian expression system, it displays identical kinetic and pharmacological features as the untagged, wild-type protein [12,37]. The yeast-expressed protein shows an apparent M_r similar to that of the unglycosylated form of the transporter (45 kDa, Fig. 2A, lanes 1 and 4). The 45 kDa polypeptide detected above with an antibody against the HA epitope located at the N-terminus is not a proteolytic fragment, since the protein detected with an antibody against the C-terminus displays the same molecular mass (see Fig. 1A, lane 4). As shown in Fig. 2A, the size of the yeast-expressed protein (lane 4) corresponds to the size of the unglycosylated mutant ('Triple', lane 3) and to the wild-type protein produced in presence of tunicamycin in a mammalian system (lane 4), (see also [12]).

3.3. The expression $rVMAT_1$ is enhanced at low temperatures

We have shown that glycosylation is not required for $rVMAT_1$ activity in a mammalian system [12]. The mutant $rVMAT_1$ in which all glycosylation sites have been mutated away retains the ability to protect mammalian cells against the toxicity of MPP^+ [12]. Yet, in the case of the yeast-expressed $rVMAT_1$, it fails to confer resistance to MPP^+ to strains YAE65 and YHE4 which are particularly sensitive to the toxin [20,22]. In addition, membranes prepared from yeast expressing $rVMAT_1$ do not catalyze neither serotonin transport nor reserpine binding (not shown). It has been suggested that *N*-linked glycosylation serves, among other functions, as quality control device for correct protein folding in the endoplasmic reticulum (ER) [43]. $rVMAT_1$ is probably not glycosylated in yeast because of improper folding. Since protein folding and stability are often favored under low temperatures, *S. cerevisiae* was grown at different temperatures and the effect on the processing of $rVMAT_1$ was investigated. As shown in Fig. 2B, $rVMAT_1$ expression was highly influenced by the temperature of cultivation. As tem-

peratures decreased (24°C and 16°C) expression levels significantly increased. Furthermore, at 16°C a large fraction of the expressed $rVMAT_1$ underwent core glycosylation. As seen in Fig. 2B, lane 5, a distinct band with an apparent molecular mass of ~53 kDa is clearly recognized. This band corresponds to the core-glycosylated form usually seen using the T7 polymerase/*Vaccinia* virus expression system (see Fig. 2A, lane 1) [12]. The bands seen at ~87 kDa correspond to oligomeric forms of VMAT. Upon treatment with *N*-glycosidase F (PNGase-F), the band coinciding with the glycosylated form disappears, whereas the lower unglycosylated form remains intact (not shown). The results imply that under the low-temperature conditions the transporter is post-translationally modified.

3.4. The intracellular distribution of VMAT is not altered at different temperatures

To follow the above findings, the intracellular distribution of the transporter at various growth temperatures was tested. For this purpose, a functional chimera between the tagged $rVMAT_1$ and the green fluorescent protein was prepared (HA-$rVMAT_1$-GFP). Notably, the pattern of HA-$rVMAT_1$-GFP fluorescence distribution was virtually identical at either 30°C or 14°C (shown in green, Fig. 3, 30°C or 14°C). Indicating that although at lower temperatures $rVMAT_1$ undergoes core-glycosylation, the transporter is still targeted to the same organelle. The punctate pattern corresponding to the chimeric transporter is present uniformly in the cell and re-

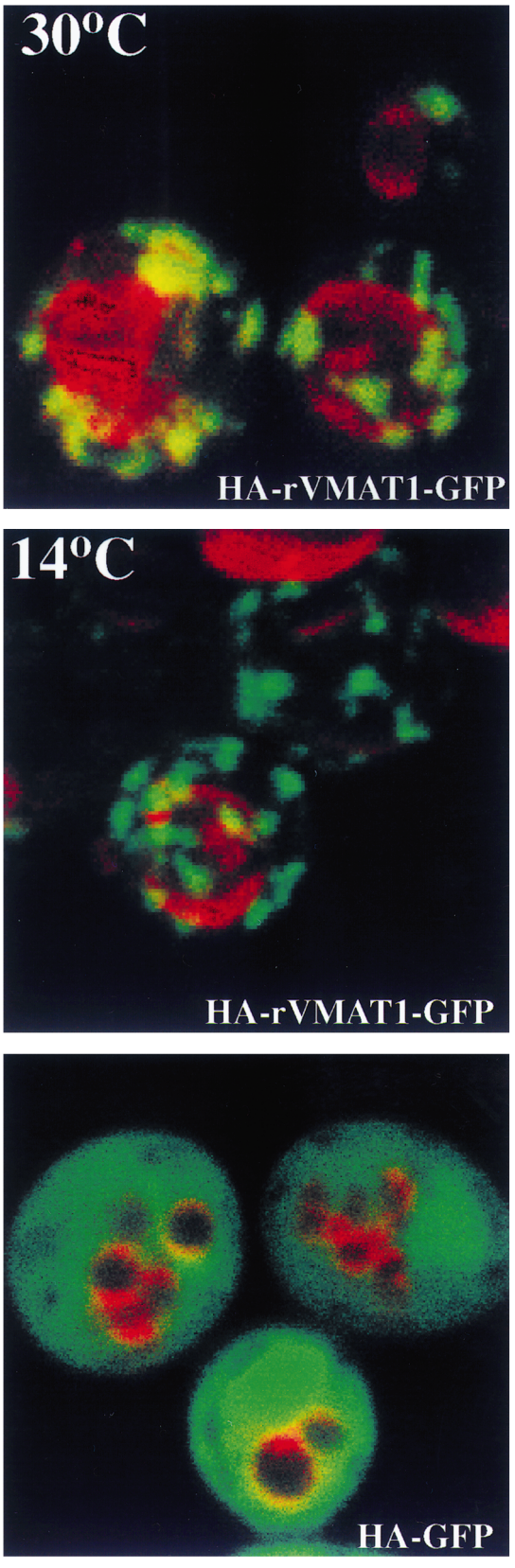

→

Fig. 3. The intracellular distribution of $rVMAT_1$ remains invariable at the different growth temperatures. A chimera between $rVMAT_1$ and the green fluorescent protein (GFP) was prepared to follow the distribution of the transporter in living cells. Yeast cells were grown at 30°C and 16°C, stained with the vacuolar marker FM4-64 and visualized with a confocal microscope. Fluorescence corresponding to the GFP is shown in green, while that of the FM4-64 dye is shown in red. The pattern of fluorescence of the $rVMAT_1$-GFP chimera resembles the late-Golgi marker Kex2p [44]. A similar pattern was found for $bVMAT_2$-GFP (not shown). As a control we expressed GFP alone using the same fusion sequence. The GFP shows a clear cytoplasmic distribution (lower panel). The VMAT-GFP chimeras are completely functional in a mammalian expression system (not shown).

sembles the distribution of the late-Golgi marker Kex2p [44]. This pattern contrasts to the ring staining decoration of the vacuolar vital stain of FM4–64 (shown in red) and clearly differs from the cytoplasmic pattern found for the wild-type HA-GFP (Fig. 3, lower panel) or the vacuolar-targeted HA-EmrE-GFP transporter [20], both proteins expressed using the same N-terminal fused sequence.

3.5. Simultaneous expression of chaperones and VMAT

Our manipulations have increased the level of expression and glycosylation. Yet, the rVMAT1 expressed in yeast is still incapable of protecting the yeast cells against MPP^+, or of catalyzing transport of monoamines or binding reserpine. To improve the probability to achieve correct protein maturation we tested the effect of co-expression of mammalian calnexin (a known chaperone) together with VMAT. The co-expressed calnexin migrates in SDS–PAGE as the endogenous calnexin from cell lines CHO, CV-1 and MDCK cells (not shown). In addition to calnexin, we co-expressed Shr3p from a high copy-number plasmid [34]. Shr3p is an ER-resident yeast chaperonin shown to be essential for packaging of amino acid permeases into transport vesicles [34,45,46]. Nonetheless, cells expressing simultaneously VMAT, calnexin and Shr3p did not show enhanced resistance towards MPP^+. Membranes prepared from these cells were still unable to bind reserpine or to accumulate serotonin. We also tested the addition of substrates and ligands as they were shown to act as molecular chaperones for otherwise misfolded proteins [47,48]. Membranes from cells grown on standard medium supplemented with millimolar concentrations of serotonin or noradrenaline or micromolar concentrations of reserpine did not induce enhanced VMAT activity or protein maturation (see Fig. 2B, lane 3). Finally, no differences in $rVMAT_1$ expression were found between cells bearing or lacking the co-expressed chaperones, grown either at 30°C, 24°C or 16°C (not shown).

3.6. The yeast-expressed $bVMAT_2$ binds tetrabenazine

None of the above manipulations rendered a protein capable of transporting serotonin in a proton-dependent manner. This activity requires proper assembly into a proton impermeable membrane and may even require specific lipids. Therefore binding of [^{3}H]dihydrotetrabenazine ([^{3}H]TBZOH), a partial activity detected even in detergent (see below) was measured. As already stated, tetrabenazine binds to and inhibits $VMAT_2$ at nanomolar concentrations while concentrations as high as 20 μM do not affect transport mediated by $VMAT_1$ [7]. The gene encoding $bVMAT_2$ [49] was inserted in the plasmid BFG-1 at the *Not*I site. Since we intended to purify the expressed protein, a polyhistidine (His_6) tag was engineered by PCR at the carboxy terminus, this protein was also referred to as HA-$bVMAT_2$-His. Taking into consideration our previous results, the 3′-UTR of $rVMAT_1$ was included in this construct to stabilize the mRNA transcript and to achieve efficient expression. The yeast expressed $bVMAT_2$ displays a mobility similar to the fully functional protein expressed using the T7 Polymerase/Vaccinia virus expression system suggesting similar glycosylation levels (see Fig. 2A, lanes 5 and 6). The expression levels and the degree of glycosylation of $bVMAT_2$ were much less sensitive to the growth temperature than those of $rVMAT_1$ (data not shown). As shown in Fig. 4A, membranes prepared from cells expressing $bVMAT_2$ (closed bars) but not $rVMAT_1$ (open bars), display high-affinity [^{3}H]dihydrotetrabenazine binding. When the specific binding was analyzed using the method of Scatchard, a linear plot was obtained suggesting the presence of a single species of binding sites. The K_d calculated for the yeast-expressed $bVMAT_2$ was 15.3 nM and the B_{max} was 13.7 pmol/mg, whereas the K_d for the CHO-expressed $bVMAT_2$ was 29.5 nM and the B_{max} was 73.2 pmol/mg. The measured constants were in good agreement with the values found for the native protein in the literature [40]. From the measured number of binding sites, we estimate about 15 000–20 000 copies of $bVMAT_2$ per cell. The expression level of $rVMAT_1$ was in the same order of magnitude, as estimated from quantitative Western blots. As in the native protein, [^{3}H]TBZOH binding to the yeast-expressed $bVMAT_2$ was sensitive to nanomolar concentrations of ketanserin but barely inhibited by micromolar concentrations of reserpine, millimolar concentrations of serotonin or noradrenaline (not

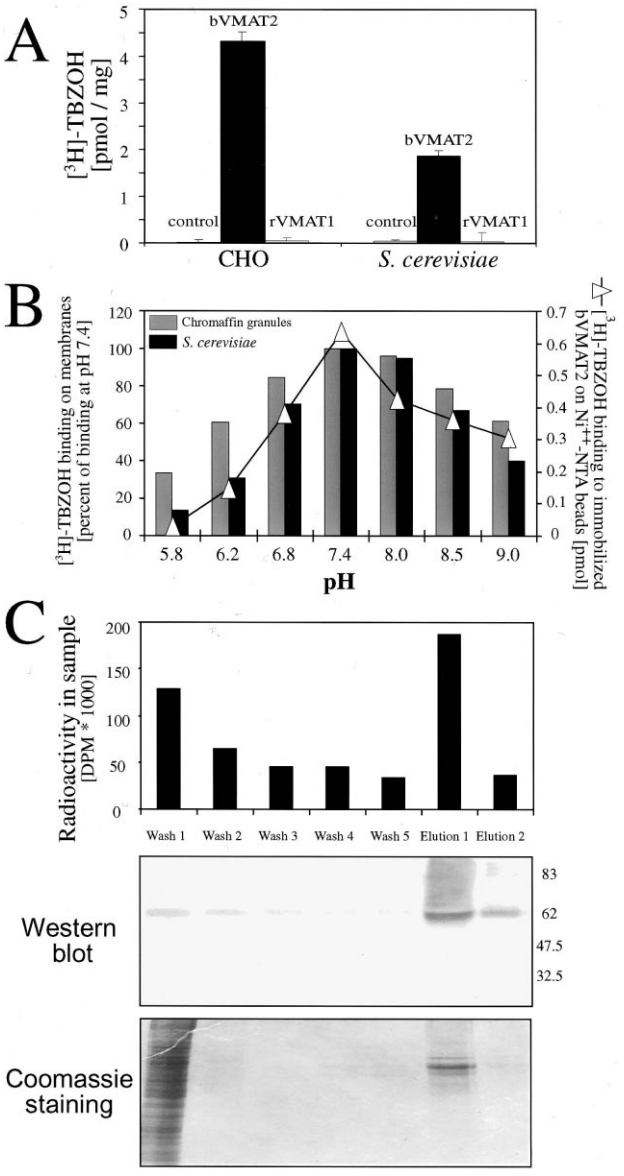

Fig. 4. (A) Binding of [^{3}H]dihydrotetrabenazine to bVMAT$_2$. Membranes prepared from CHO and *S. cerevisiae* expressing either rVMAT$_1$ or bVMAT$_2$ were tested for [^{3}H]TBZOH binding as described in Section 2. Binding was performed in triplicate and allowed for 10 min at room temperature. (B) The solubilized bVMAT$_2$, immobilized on Ni^{2+}-NTA beads shows the same pH dependence of [^{3}H]TBZOH binding as the native protein from bovine chromaffin granules. Bovine chromaffin granules (gray bars) and membranes from yeast-expressing bVMAT$_2$ (black bars) were assayed for [^{3}H]TBZOH binding using buffered solutions titrated to different pHs as described in Section 2. A similar pH-dependence was found for the recombinant and the native protein. In a separate experiment, membranes from yeast expressing bVMAT$_2$ were solubilized and allowed to bind to Ni^{2+}-NTA beads as described in Section 2. Beads were washed and assayed for [^{3}H]TBZOH binding at different pHs (open triangles). The amount of binding was normalized according to the protein retained at the beads. Control experiments using membranes from non-expressing cells showed no significant binding above background (not shown). (C) Purification of bVMAT$_2$ using Ni^{2+}-NTA beads. The complex [^{3}H]TBZOH-bVMAT$_2$ was used to follow the bVMAT$_2$ during the purification process. Membranes were labeled with [^{3}H]TBZOH, solubilized, allowed to bind to Ni^{2+}-NTA beads, and mounted on a mini-column. The column was washed several times and the protein was eluted with 200 mM imidazole. The radioactivity of the fractions was assessed using scintillation counting. The presence of bVMAT$_2$ in the different fractions was tested using Western blots (middle panel). A similar gel was prepared and stained with coomassie blue (lower panel). For experimental details see Section 2.

→

shown). In addition, the binding did not depend on an imposed proton gradient as the reactions were performed in the absence of ATP. The binding of [^{3}H]TBZOH to chromaffin granules shows a distinctive pH dependence [50]. As shown in Fig. 4B (bars), the binding of [^{3}H]TBZOH to chromaffin granules (gray bars) is low at acidic pH (5.8) and increases to its maximum at pH 7.4–8.0, whereas at more basic conditions it begins to decline. An analogous behavior was measured for the yeast expressed bVMAT$_2$ (see Fig. 4B, dark bars). Our results are essentially the same as found by Scherman and Henry [50], except that in our hands binding decreases at alkaline pH. Based on the results presented here, we conclude that the binding of tetrabenazine in the yeast-expressed bVMAT$_2$ resembles that in the native transporter from bovine chromaffin granules.

3.7. [^{3}H]TBZOH binding to a detergent-solubilized immobilized bVMAT$_2$

Recently a convenient assay for high-affinity ligand binding in a detergent solubilized transporter was introduced [51]. This assay takes advantage of the ability to immobilize His$_6$-tagged proteins on Ni^{2+}-NTA beads. We adapted this assay to assess TBZOH binding on the detergent-solubilized bVMAT2 anchored on the metal chelate adsorbent (Ni^{2+}-NTA beads). We found that dodecyl maltoside (DM) is appropriate for solubilizing bVMAT$_2$ in a

form that retains high [^{3}H]TBZOH binding activity. Yeast membranes previously labeled with 15 nM [^{3}H]TBZOH were solubilized using 0.5% DM (or a combination of 0.5% DM and 0.25% cholate). [^{3}H]TBZOH remains associated with the solubilized bVMAT$_2$ as judged by the fact that the majority of the radioactivity released to the supernatant could be subsequently bound to Ni^{2+}-NTA beads. Conversely, it was possible to assay [^{3}H]TBZOH binding on solubilized bVMAT$_2$ and immobilized on Ni^{2+}-NTA beads. The binding was dependent on the presence of bVMAT$_2$ and could be competed away by excess of unlabeled tetrabenazine or ketanserin. In agreement with previous findings [52], increasing concentrations of cholate (up to 1.5%) caused the gradual loss of bound [^{3}H]TBZOH. Also, Triton X-100 was found deleterious for [^{3}H]TBZOH binding activity [52]. This effect is reversible since upon exchange with 0.5% DM the binding activity is recovered. Importantly, the immobilization assay gives an excellent signal-to-noise ratio since the beads can be washed several times without loosing significant counts. To test whether the immobilized bVMAT$_2$ exhibits the characteristics of the membrane inserted protein, we examined also the pH dependence of [^{3}H]TBZOH binding. The results shown in Fig. 4B (triangles) demonstrate that the immobilized bVMAT$_2$ reproduces the pH dependence of [^{3}H]TBZOH of the protein in the membrane.

3.8. Purification of the [^{3}H]TBZOH binding activity

To purify rVMAT1 expressed in mammalian cells we used immobilized metal affinity chromatography [37]. Using a similar approach that takes advantage of its robust [^{3}H]TBZOH binding activity we purified the yeast expressed bVMAT$_2$. Membranes were first labeled with [^{3}H]TBZOH, and then solubilized with DM and cholate. Since [^{3}H]TBZOH remained bound after solubilization, it was possible to follow the protein during the purification process assessing the radioactivity associated with the different fractions (see Fig. 4C). The radioactivity found in the void volume and the initial washes of the column, represents [^{3}H]TBZOH non-specifically bound to proteins or released upon solubilization. Using immunoblots some bVMAT$_2$ was also detected in fractions corresponding to non-stringent washes (Fig. 4C, lower panel wash 1–5). The bulk of the specific [^{3}H]TBZOH binding activity remained bound to the beads and was released only in the presence of 200 mM imidazole (see Fig. 4C, elution 1). When the eluted fractions were resolved on SDS–PAGE and stained with coomassie blue, a predominant band with a size of $\sim$63 kDa was detected (Fig. 4C lower panel). A single band with a similar size was specifically identified by Western blot (see Fig. 4C, middle panel, elution 1) suggesting that the major band was bVMAT$_2$.

4. Discussion

Vesicular monoamine transporters (VMATs) are H^+-driven antiporters that catalyze the transport of biogenic amines across membranes of secretory organelles. The mechanism of transport remains obscure, largely because of the lack of suitable expression systems which provide large amount of protein for biochemical and crystallographic characterization. High-level expression of functional polytopic membrane proteins is a difficult task due to the problems that arise regarding efficient protein folding and stability. In this report we describe the first detailed attempt to express vesicular monoamine transporters in the yeast *S. cerevisiae*. After several futile attempts to express rVMAT$_1$ using the endogenous codon for initiation of translation, elevated expression was achieved only after modification of the codon usage of the initiation region. Instead of substituting the hampering codons for the yeast-preferred ones, short and readily translatable sequences were fused in frame immediately before the first methionine of the protein. As a result a drastic increase in the expression was obtained. The levels of expression increased together with the length of the fused sequence. The use of synonymous codons is strongly biased in the yeast *S. cerevisiae* [36]; a major determinant of this bias is the abundance of the different tRNA species [53]. Evidently, protein synthesis is more efficient when the pool of the required tRNAs is not limiting. Besides, effective translation probably confers increased stability to the mRNA transcript. Therefore, preferred codons improve protein expression and favor mRNA stability.

The 5′-UTR sequences may affect the efficiency of

protein synthesis. In the case of $rVMAT_1$, the differences in expression levels cannot be explained by this factor: two plasmids with identical 5′-UTR but varying only in the fused translated sequences express rVMAT1 at very different levels. Furthermore, we showed that fusion of the longer sequence was sufficient to procure high expression of $bVMAT_2$ (this work), the green fluorescent protein (GFP) and the *E. coli* multidrug transporter EmrE [20]. Finally, we also found that apart from the effect of the codon usage at the N-terminus, the 3′-untranslated region of $rVMAT_1$ was critical for expression. This region contains the mammalian polyadenylation signal and may serve as stabilizing factor for the mRNA transcript, therefore promoting efficient expression.

$rVMAT_1$ was expressed at relatively high levels, yet the size of the protein corresponded to the size of the non-glycosylated form. Lack of glycosylation is usually correlated with misfolding of proteins. We deduced that rVMAT1 is incorrectly folded as no significant activity was detected in a variety of assays that test established traits of the functional transporter. Low cultivation temperatures caused a remarkable increase in the levels of expression. Furthermore, under these conditions about half of the expressed rVMAT1 underwent core glycosylation. This post-translational modification, not occurring at 30°C, indicates that a specific folding event was accomplished. Yet, additional steps leading towards genuine conformation are necessary since activity was still not detected. As judged by chimeras with the GFP, the intracellular distribution of $rVMAT_1$ (and although not shown also of $bVMAT_2$), remained unchanged either at 30°C or 14°C, conditions at which $rVMAT_1$ undergoes core glycosylation. The punctate pattern of fluorescence resembles the late-Golgi compartment. The acquisition of a correct three-dimensional conformation in the ER is not a spontaneous, unassisted event. The ER contains a variety of molecular chaperones and foldases involved in the folding and maturation process [54]. Since the endogenous yeast chaperones may not recognize mammalian misfolded proteins, we co-expressed canine calnexin together with VMAT. Calnexin was initially chosen as it was found to be the chaperone causing the maximal increase in the level of functional heterologously-expressed plasma-membrane serotonin transporter (SERT) [55]. Although the yeast-expressed calnexin showed mobility similar to that of the endogenously expressed mammalian counterpart, its expression was ineffectual regarding the production of functional $rVMAT_1$ or $bVMAT_2$. In contrast to $rVMAT_1$, the expression levels of $bVMAT_2$ were only slightly affected by the growth temperature.

Using membrane preparations from *S. cerevisiae* expressing $bVMAT_2$, it was possible to measure high-affinity specific dihydrotetrabenazine ([^{3}H]-TBZOH) binding. The binding properties shown by the heterologously expressed $bVMAT_2$ were similar to those found in the native chromaffin granule transporter. Only ketanserin and tetrabenazine completely abolished [^{3}H]TBZOH binding, whereas exceedingly high concentrations of reserpine and substrates of transport modestly inhibited the reaction. In addition, the distinctive pH dependence of [^{3}H]TBZOH binding known for the native protein was detected also in the yeast-expressed $bVMAT_2$. Based on the ability of dodecyl maltoside to solubilize $bVMAT_2$ in a form that retains [^{3}H]TBZOH binding activity, a novel binding assay was developed. The assay takes advantage of a poly-histidine tag engineered at the C-terminus of $bVMAT_2$ and a metal chelate adsorbent (Ni^{2+}-NTA beads). The immobilized $bVMAT_2$ displays the same features of the membrane protein regarding the affinity to [^{3}H]TBZOH, the pharmacological profile and the pH dependence of binding.

It was previously shown that it is possible to use the Ni^{2+}-NTA resin to purify the transporter [37,56]. In this communication we exploited the robust [^{3}H]TBZOH binding to follow the protein during the purification procedure directly assessing the radioactivity at each fraction. Although a supplementary chromatographic step is required to obtain pure preparations of the protein, a notable enrichment is achieved using a single Ni^{2+}-NTA column.

Sievert and collaborators have expressed $rVMAT_2$ using baculovirus-infected insect cells [56]. The expressed protein display [^{125}I]AZIK (7-azido-8-[^{125}I]iodoketanserin) and [^{3}H]TBZOH binding activity, yet no transport activity or reserpine binding were shown. In our hands $rVMAT_1$ expressed in this system shows neither of these activities albeit elevated levels of expression (RY and SS, unpublished observations).

In this work we developed general strategies for expression of heterologous proteins in yeast: namely, fusion to readily translatable sequences having codons preferred by yeast and growth at low temperatures. Yet, the results illustrate the difficulties to express fully functional vesicular monoamine transporters perhaps due to the complex folding of these proteins or the lack unknown essential factors. Strikingly, the native binding site for tetrabenazine and ketanserin is formed using different heterologous expression systems. The results imply that its correct assembly is less dependent on the folding machinery. We therefore propose the possibility that the creation of the binding site demands fewer adjacent domains within the protein or it is composed by determinants located within the same region of the polypeptide. In contrast, the reserpine and substrate binding site requires a more delicate arrangement. This site is directly affected by the H^+-electrochemical gradient since it drives the refolding needed to accelerate the binding of reserpine and to catalyze the whole transport process.

Acknowledgements

The authors would like to thank Sonia Mordoch and Dvir Rotem for the help given at several stages of this work. We thank also Dr Chris Tate and Dr Per Ljungdahl for fruitful discussion, and Dr Aryeh Weiss for the technical assistance on the confocal microscopy. This work was performed in the Charles Smith Laboratory for Collaborative Research. It was supported by grants from the Deutsche–Israeli Program (Federal Ministry of Education, Science and Research-BMBF-International Bureau at the German Aerospace Center Technology) and Grant NS16708 from the National Institutes of Health.

References

[1] S. Schuldiner, A. Shirvan, M. Linial, Vesicular neurotransmitter transporters: from bacteria to humans, Physiol. Rev. 75 (1995) 369–392.

[2] Y. Stern-Bach, N. Greenberg-Ofrath, I. Flechner, S. Schuldiner, Identification and purification of a functional amine transporter from bovine chromaffin granules, J. Biol. Chem. 265 (1990) 3961–3966.

[3] M. Vincent, J. Near, Purification of a [^{3}H]dihydrotetrabenazine-binding protein from bovine adrenal medulla, Mol. Pharmacol. 40 (1991) 889–894.

[4] M.F. Isambert, B. Gasnier, D. Botton, J.P. Henry, Characterization and purification of the monoamine transporter of bovine chromaffin granules, Biochemistry 31 (1992) 1980–1986.

[5] Y. Liu, D. Peter, A. Roghani, S. Schuldiner, G. Prive, D. Eisenberg, N. Brecha, R. Edwards, A cDNA that suppresses MPP+ toxicity encodes a vesicular amine transporter, Cell 70 (1992) 539–551.

[6] J. Erickson, L. Eiden, B. Hoffman, Expression cloning of a reserpine-sensitive vesicular monoamine transporter, Proc. Natl. Acad. Sci. USA 89 (1992) 10993–10997.

[7] D. Peter, J. Jimenez, Y. Liu, J. Kim, R.H. Edwards, The chromaffin granule and synaptic vesicle amine transporters differ in substrate recognition and sensitivity to inhibitors, J. Biol. Chem. 269 (1994) 7231–7237.

[8] A. Shirvan, O. Laskar, S. Steiner-Mordoch, S. Schuldiner, Histidine-419 plays a role in energy coupling in the vesicular monoamine transporter from rat, FEBS Lett. 356 (1994) 145–150.

[9] S. Steiner-Mordoch, A. Shirvan, S. Schuldiner, Modification of the pH profile and tetrabenazine sensitivity of rat VMAT1 by replacement of aspartate 404 with glutamate, J. Biol. Chem. 271 (1996) 13048–13054.

[10] A. Merickel, P. Rosandich, D. Peter, R. Edwards, Identification of residues involved in substrate recognition by a vesicular monoamine transporter, J. Biol. Chem. 270 (1995) 25798–25804.

[11] A. Merickel, H.R. Kaback, R.H. Edwards, Charged residues in transmembrane domains ii and xi of a vesicular monoamine transporter form a charge pair that promotes high affinity substrate recognition, J. Biol. Chem. 272 (1997) 5403–5408.

[12] R. Yelin, S. Steiner-Mordoch, B. Aroeti, S. Schuldiner, Glycosylation of a vesicular monoamine transporter: a mutation in a conserved proline residue affects the activity, glycosylation, and localization of the transporter, J. Neurochem. 71 (1998) 2518–2527.

[13] W.B. Frommer, O. Ninnemann, Heterologous expression of genes in bacterial, fungal, animal, and plant cells, Annu. Rev. Plant Physiol. Plant Mol. Biol. 46 (1995) 419–444.

[14] N. Sauer, R. Stadler, A sink-specific H+/monosaccharide cotransporter from *Nicotiana tabacum*: cloning and heterologous expression in baker's yeast, Plant J. 4 (1993) 601–610.

[15] N. Sauer, J. Stolz, SUC1 and SUC2: two sucrose transporters from *Arabidopsis thaliana*; expression and characterization in baker's yeast and identification of the histidine-tagged protein, Plant J. 6 (1994) 67–77.

[16] W.B. Frommer, S. Hummel, D. Rentsch, Cloning of an Arabidopsis histidine transporting protein related to nitrate and peptide transporters, FEBS Lett. 347 (1994) 185–189.

[17] P. Sander, S. Grunewald, M. Bach, W. Haase, H. Reilander, H. Michel, Heterologous expression of the human D2S dop-

amine receptor in protease-deficient *Saccharomyces cerevisiae* strains, Eur. J. Biochem. 226 (1994) 697–705.
[18] M. Raymond, S. Ruetz, D.Y. Thomas, P. Gros, Functional expression of P-glycoprotein in *Saccharomyces cerevisiae* confers cellular resistance to the immunosuppressive and antifungal agent FK520, Mol. Cell. Biol. 14 (1994) 277–286.
[19] D.L. Hogue, L. Kerby, V. Ling, A mammalian lysosomal membrane protein confers multidrug resistance upon expression in *Saccharomyces cerevisiae*, J. Biol. Chem. 274 (1999) 12877–12882.
[20] R. Yelin, D. Rotem, S. Schuldiner, EmrE, a small Escherichia coli multidrug transporter, protects Saccharomyces cerevisiae from toxins by sequestration in the vacuole, J. Bacteriol. 181 (1999) 949–956.
[21] D. Hanahan, Studies on transformation of *Escherichia coli* with plasmids, J. Mol. Biol. 166 (1983) 557–580.
[22] A.E. Ehrenhofer-Murray, F.E. Wurgler, C. Sengstag, The *Saccharomyces cerevisiae* SGE1 gene product: a novel drug-resistance protein within the major facilitator superfamily, Mol. Gen. Genet. 244 (1994) 287–294.
[23] A.E. Ehrenhofer-Murray, M.U. Seitz, C. Sengstag, The Sge1 protein of Saccharomyces cerevisiae is a membrane-associated multidrug transporter, Yeast 14 (1998) 49–65.
[24] R.K. Nakamoto, R. Rao, C.W. Slayman, Expression of the yeast plasma membrane [H^+]ATPase in secretory vesicles. A new strategy for directed mutagenesis., J. Biol. Chem. 266 (1991) 7940–7949.
[25] C. Guthrie, G. Fink, Guide to yeast genetics and molecular biology, Methods Enzymol. 194 (1991) 1.
[26] R. Elble, A simple and efficient procedure for transformation of yeast, Biotechniques 13 (1992) 18–20.
[27] R. Ballester, T. Michaeli, K. Ferguson, H.P. Xu, F. McCormick, M. Wigler, Genetic analysis of mammalian GAP expressed in yeast, Cell 59 (1989) 681–686.
[28] J.M. Villalba, M.G. Palmgren, G.E. Berberian, C. Ferguson, R. Serrano, Functional expression of plant plasma membrane H(+)-ATPase in yeast endoplasmic reticulum, J. Biol. Chem. 267 (1992) 12341–12349.
[29] M. Johnston, R.W. Davis, Sequences that regulate the divergent GAL1-GAL10 promoter in *Saccharomyces cerevisiae*, Mol. Cell. Biol. 4 (1984) 1440–1448.
[30] R.S. Sikorski, P. Hieter, A system of shuttle vectors and yeast host strains designed for efficient manipulation of DNA in *Saccharomyces cerevisiae*, Genetics 122 (1989) 19–27.
[31] I.A. Wilson, H.L. Niman, R.A. Houghten, A.R. Cherenson, M.L. Connolly, R.A. Lerner, The structure of an antigenic determinant in a protein, Cell 37 (1984) 767–778.
[32] I. Wada, D. Rindress, P.H. Cameron, W.J. Ou, J.J.d. Doherty, D. Louvard, A.W. Bell, D. Dignard, D.Y. Thomas, J.J. Bergeron, SSR alpha and associated calnexin are major calcium binding proteins of the endoplasmic reticulum membrane, J. Biol. Chem. 266 (1991) 19599–19610.
[33] M. Schena, D. Picard, K.R. Yamamoto, Vectors for constitutive and inducible gene expression in yeast, Methods Enzymol. 194 (1991) 389–398.
[34] P.O. Ljungdahl, C.J. Gimeno, C.A. Styles, G.R. Fink, SHR3: a novel component of the secretory pathway specifically required for localization of amino acid permeases in yeast, Cell 71 (1992) 463–478.
[35] S. Rees, J. Coote, J. Stables, S. Goodson, S. Harris, M. Lee, Bicistronic vector for the creation of stable mammalian cell lines that predisposes all antibiotic-resistant cells to express recombinant protein, Biotechniques 20 (1996) 102–104.
[36] J.L. Bennetzen, B.D. Hall, Codon selection in yeast, J. Biol. Chem. 257 (1982) 3026–3031.
[37] R. Yelin, S. Schuldiner, Purification of vesicular monoamine transporters: from classical techniques to histidine tags, Methods Enzymol. 296 (1998) 64–72.
[38] D. Prasher, V. Eckenrode, W. Ward, F. Prendergast, M. Cormier, Primary structure of the Aequoria victoria green-fluorescent protein, Gene 111 (1992) 229–233.
[39] R. Heim, A. Cubitt, R. Tsien, Improved green fluorescence, Nature 373 (1995) 663–664.
[40] D. Scherman, P. Jaudon, J.P. Henry, Characterization of the monoamine carrier of chromaffin granule membrane by binding of [2-^{3}H]dihydrotetrabenazine, Proc. Natl. Acad. Sci. USA 80 (1983) 584–588.
[41] A. Hoekema, R.A. Kastelein, M. Vasser, H.A. de Boer, Codon replacement in the PGK1 gene of *Saccharomyces cerevisiae*: experimental approach to study the role of biased codon usage in gene expression, Mol. Cell. Biol. 7 (1987) 2914–2924.
[42] P.M. Sharp, T.M. Tuohy, K.R. Mosurski, Codon usage in yeast: cluster analysis clearly differentiates highly and lowly expressed genes, Nucleic Acids Res. 14 (1986) 5125–5143.
[43] E.S. Trombetta, A. Helenius, Lectins as chaperones in glycoprotein folding, Curr. Opin. Struct. Biol. 8 (1998) 587–592.
[44] S.F. Nothwehr, E. Conibear, T.H. Stevens, Golgi and vacuolar membrane proteins reach the vacuole in vps1 mutant yeast cells via the plasma membrane, J. Cell Biol. 129 (1995) 35–46.
[45] M.J. Kuehn, R. Schekman, P.O. Ljungdahl, Amino acid permeases require COPII components and the ER resident membrane protein Shr3p for packaging into transport vesicles in vitro, J. Cell Biol. 135 (1996) 585–595.
[46] C.F. Gilstring, M. Melin-Larsson, P.O. Ljungdahl, Shr3p mediates specific COPII coatomer-cargo interactions required for the packaging of amino acid permeases into ER-derived transport vesicles, Mol. Biol. Cell. 10 (1999) 3549–3565.
[47] T.W. Loo, D.M. Clarke, Superfolding of the partially unfolded core-glycosylated intermediate of human P-glycoprotein into the mature enzyme is promoted by substrate-induced transmembrane domain interactions, J. Biol. Chem. 273 (1998) 14671–14674.
[48] T.W. Loo, D.M. Clarke, Correction of defective protein kinesis of human P-glycoprotein mutants by substrates and modulators, J. Biol. Chem. 272 (1997) 709–712.
[49] M. Howell, A. Shirvan, Y. Stern-Bach, S. Steiner-Mordoch, J.E. Strasser, G.E. Dean, S. Schuldiner, Cloning and functional expression of a tetrabenazine sensitive vesicular mono-

amine transporter from bovine chromaffin granules, FEBS Lett. 338 (1994) 16–22.
[50] D. Scherman, J.P. Henry, The catecholamine carrier of bovine chromaffin granules. Form of the bound amine, Mol. Pharmacol. 23 (1983) 431–436.
[51] T.R. Muth, S. Schuldiner, A membrane-embedded glutamate is required for ligand binding to the multidrug transporter EmrE, EMBO J. 19 (2000) 234–240.
[52] D. Scherman, J.P. Henry, Solubilization of the catecholamine carrier of chromaffin granule membranes in a form that binds substrates and inhibitors of uptake, Biochemistry 22 (1983) 2805–2810.
[53] M. Bulmer, Coevolution of codon usage and transfer RNA abundance, Nature 325 (1987) 728–730.
[54] D.N. Hebert, J.F. Simons, J.R. Peterson, A. Helenius, Calnexin, calreticulin, and Bip/Kar2p in protein folding, Cold Spring Harbor Symp. Quant. Biol. 60 (1995) 405–415.
[55] C.G. Tate, E. Whiteley, M.J. Betenbaugh, Molecular chaperones stimulate the functional expression of the cocaine-sensitive serotonin transporter, J. Biol. Chem. 274 (1999) 17551–17558.
[56] M.K. Sievert, D.S. Thiriot, R.H. Edwards, A.E. Ruoho, High-efficiency expression and characterization of the synaptic-vesicle monoamine transporter from baculovirus-infected insect cells, Biochem. J. 330 (1998) 959–966.